

DEEP K-BAND OBSERVATIONS OF TMC-1 WITH THE GREEN BANK TELESCOPE: DETECTION OF HC₇O, NON-DETECTION OF HC₁₁N, AND A SEARCH FOR NEW ORGANIC MOLECULES

M. A. CORDINER^{1,2}, S. B. CHARNLEY¹, Z. KISIEL³, B. A. MCGUIRE⁴, Y.-J. KUAN^{5,6}

Draft version March 25, 2022

ABSTRACT

The 100 m Robert C. Byrd Green Bank Telescope K-band (KFPA) receiver was used to perform a high-sensitivity search for rotational emission lines from complex organic molecules in the cold interstellar medium towards TMC-1 (cyanopolyynes peak), focussing on the identification of new carbon-chain-bearing species as well as molecules of possible prebiotic relevance. We report a detection of the carbon-chain oxide species HC₇O and derive a column density of $(7.8 \pm 0.9) \times 10^{11} \text{ cm}^{-2}$. This species is theorized to form as a result of associative electron detachment reactions between oxygen atoms and C₇H⁻, and/or reaction of C₆H₂⁺ with CO (followed by dissociative electron recombination). Upper limits are given for the related HC₆O, C₆O and C₇O molecules. In addition, we obtained the first detections of emission from individual ¹³C isotopologues of HC₇N, and derive abundance ratios HC₇N/HCCC¹³CCCCN = 110 ± 16 and HC₇N/HCCCC¹³CCCN = 96 ± 11 , indicative of significant ¹³C depletion in this species relative to the local interstellar elemental ¹²C/¹³C ratio of 60-70. The observed spectral region covered two transitions of HC₁₁N, but emission from this species was not detected, and the corresponding column density upper limit is $7.4 \times 10^{10} \text{ cm}^{-2}$ (at 95% confidence). This is significantly lower than the value of $2.8 \times 10^{11} \text{ cm}^{-2}$ previously claimed by Bell et al. (1997) and confirms the recent non-detection of HC₁₁N in TMC-1 by Loomis et al. (2016). Upper limits were also obtained for the column densities of malononitrile and the nitrogen heterocycles quinoline, isoquinoline and pyrimidine.

Subject headings: radio lines: ISM – ISM: abundances – ISM: lines and bands – ISM: molecules

1. INTRODUCTION

Radio spectroscopy is a powerful and rigorous technique for the detection of new molecules in the dense interstellar medium. Organic molecules are commonly observed in many different astronomical sources (Herbst & van Dishoeck 2009) and the fact that many of the known interstellar organics are also present in protoplanetary disks and in comets (*e.g.* Öberg et al. 2015; Walsh et al. 2016; Cochran et al. 2015; Biver et al. 2015; Altwegg et al. 2016) supports the view that interstellar clouds could plausibly be the first formation sites for the prebiotic molecules that may have been delivered to the early Earth by comets (*e.g.* Mumma & Charnley 2011).

The dark interstellar cloud TMC-1 has proven to be the archetype for studies of cold cloud organic chemistry (Kaifu et al. 2004; Sakai et al. 2013; McElroy et al. 2013). Observations show that the inventory of TMC-1 is dominated by long carbon chain molecules: the cyanopolyynes (HC_{2n+1}N, $n = 1, 2, 3, 4$; CH₃C₃N, CH₃C₅N), carbon chain radicals (C₂H, C₃H, C₄H, C₅H, C₆H, C₈H, C₂N, C₃N, C₅N) and related anions, linear carbenes (H₂CCC, H₂CCCC, H₂CCCCC), polyacetylenic molecules (CH₃C₂H, CH₃C₄H) and smaller ring molecules such as *c*-C₃H and *c*-C₃H₂ (Gratier et al. 2016; Ohishi 2016).

Cyanodecapentayne (HC₁₁N) has long been considered as the largest gas-phase molecule identified in dense interstellar clouds. The first reported measurement of HC₁₁N in TMC-1 was by Bell et al. (1997), who detected two apparent transitions ($J = 39 - 38$ and $J = 38 - 37$) in the Ku band using the NRAO 140-foot telescope, from which they derived a column density of $2.8 \times 10^{11} \text{ cm}^{-2}$ (assuming a rotational temperature of 10 K). However, there have since been no reported confirmations of HC₁₁N in the literature, either in TMC-1 or any other astronomical object. Loomis et al. (2016) searched for and failed to detect six transitions of HC₁₁N in the Ku band in TMC-1 using the Green Bank Telescope (GBT), including the $J = 39 - 38$ and $J = 38 - 37$ transitions claimed by Bell et al. (1997). They obtained a (2σ) column density upper limit of $9.4 \times 10^{10} \text{ cm}^{-2}$, and concluded that the relative lack of HC₁₁N compared with the smaller cyanopolyynes may be due to the propensity of carbon chains longer than 10 C-atoms to form closed ring structures.

TMC-1 also contains shorter carbon-chains with O and S terminations: C₂O, C₃O, C₂S, C₃S (Ohishi et al. 1991; Kaifu et al. 2004). Theoretical models of interstellar anion chemistry have predicted that longer carbon-chain oxides could be present in TMC-1. Cordiner & Charnley (2012) predicted detectable column densities for C₆O, HC₆O, C₇O and HC₇O in dense interstellar clouds, where they were theorised to form as a result of associative electron detachment (AED) reactions between carbon chain anions (H)C_n⁻ and atomic oxygen. Such reactions have been observed in the laboratory by Eichelberger et al. (2007), and although these reactions were found to be rapid, the product branching ratios are currently unknown. McGuire et al. (2017a) considered the production of HC_nO radicals ($n = 3 - 7$) based on a chemistry initiated by radiative association reactions between hydrocarbon cations and CO. The importance of these reaction mechanisms can be assessed by searching for, and measuring the abundances of,

martin.cordiner@nasa.gov

¹ Astrochemistry Laboratory and the Goddard Center for Astrobiology, NASA Goddard Space Flight Center, 8800 Greenbelt Road, MD 20771, USA.

² Institute for Astrophysics and Computational Sciences, The Catholic University of America, Washington, DC 20064, USA.

³ Institute of Physics, Polish Academy of Sciences, Al. Lotnikow 32/46, 02-668 Warszawa, Poland.

⁴ National Radio Astronomy Observatory, Charlottesville, VA 22903, USA.

⁵ National Taiwan Normal University, Taipei 116, Taiwan, ROC.

⁶ Institute of Astronomy and Astrophysics, Academia Sinica, Taipei 106, Taiwan, ROC.

the predicted carbon chain oxide molecules.

Aromatic compounds play a fundamental role in prebiotic chemistry (*e.g.* Ehrenfreund et al. 2006). However, despite strong observational evidence for their presence in high-excitation astronomical environments via infrared emission (Tielens 2008), there have been no firm spectroscopic identifications of specific polycyclic aromatic hydrocarbon (PAH) molecules in the interstellar medium so far. Aromatic nitrogen heterocycles are of particular prebiotic importance and, in particular, pyrimidine could be a possible precursor of DNA nucleobases. Experiments have shown that energetic processing of interstellar ice analogues containing pyrimidine can form the nucleobases uracil, thymine and cytosine (Materese et al. 2013; Nuevo et al. 2014), as well as the N-heterocycles quinoline and isoquinoline (Materese et al. 2015). As a permanent electric dipole moment results from the presence of a heteroatom in the aromatic structure, rotational transitions are possible, however such heterocycles have not yet been detected, despite dedicated searches in star-forming regions and circumstellar envelopes (Kuan et al. 2003; Charnley et al. 2005; Brünken et al. 2006).

Experimental and theoretical studies indicate that gas-phase formation of pyrimidine and benzene could be viable in dark clouds (Bera et al. 2009; Jones et al. 2011). The recent discovery of benzene and naphthalene in the volatile ices of comet 67P (Altwegg, K., private communication 2016) provides impetus to renew searches for aromatic interstellar compounds.

During preparation of this article, McGuire et al. (2017a) published a detection of the carbon chain oxide HC₅O in TMC-1 using the GBT K-band receiver, as well as a tentative detection of HC₇O. The first detection of benzonitrile (C₆H₅CN) has also been submitted for publication (McGuire et al. 2017b)

In this paper we report detections and column densities for HC₇O and two isotopologues of HC₇N. We also report non-detections of HC₁₁N, HC₆O, C₆O, C₇O, malononitrile, quinoline, isoquinoline and pyrimidine, for which column density upper limits are presented.

2. OBSERVATIONS

Spectra were obtained towards the TMC-1 cyanopolyne peak (at J2000 R.A. 04:41:42, decl. +25:41:27) using the Robert C. Byrd Green Bank Telescope (GBT) in October–November 2011. Observations were conducted using the central beam of the K-band focal plane array (KFPA) receiver, with a half-power beam width of $\approx 37''$ on the sky. The GBT spectrometer was configured with a channel width of 12.2 kHz and 4×50 MHz spectral windows. As a result of the GBT’s dynamic scheduling system, observations were performed under consistently good weather conditions, with system temperatures (T_{sys}) in the range 35–50 K and zenith opacities 0.02–0.05. Pointing was checked every 1–2 hours, and the mean pointing error over the 64 hours allocated to our program was $5.2''$. Spectra in the range 18.1–19.8 GHz were obtained using frequency switching, and the range 20.2–20.5 GHz was observed by position switching, using an uncontaminated reference position offset by $17''$ NE from the cyanopolyne peak.

Data reduction was performed using the GBTIDL software, which included opacity correction, frequency-alignment of individual scans in the LSR frame and T_{sys} -weighted averaging. Reduced spectra were subsequently corrected for the main beam efficiency of 0.92. On-source integration times ~ 10 hours per spectral setting resulted in RMS noise lev-

TABLE 1
TARGETED LINE FREQUENCIES, TRANSITIONS AND UPPER-STATE ENERGIES

Rest Freq. (MHz)	Species	Transition	E_u (K)
18106.283	HC ₇ O	17–16 e	7.5
18106.312	HC ₇ O	16–15 e	7.5
18107.873	HC ₇ O	17–16 f	7.5
18107.900	HC ₇ O	16–15 f	7.5
18334.033	C ₇ O	16–15	7.5
18596.764	HC ₁₁ N	55–54	25.0
18638.616	HC ₅ N	7–6	3.6
18828.319	HC ₆ O	12–11 e	5.5
18828.336	HC ₆ O	11–10 e	5.5
18829.311	HC ₆ O	12–11 f	5.5
18829.327	HC ₆ O	11–10 f	5.5
18992.942	C ₉ H ₇ N	10 _{0,10} –9 _{0,9} , $F = 10-9$	5.2
18992.990	C ₉ H ₇ N	10 _{0,10} –9 _{0,9} , $F = 9-8$	5.2
18993.002	C ₉ H ₇ N	10 _{0,10} –9 _{0,9} , $F = 11-10$	5.2
19071.386	C ₆ O	11 ₁₂ –10 ₁₁	5.9
19203.671	HC ₇ O	18–17 e	8.4
19203.699	HC ₇ O	17–16 e	8.4
19205.267	HC ₇ O	18–17 f	8.4
19205.294	HC ₇ O	17–16 f	8.4
19479.903	C ₇ O	17–16	8.4
19785.41	CH ₂ (CN) ₂	4 _{1,3} –4 _{0,4}	3.6
20278.94	C ₄ H ₄ N ₂	12 _{9,3} –12 _{8,4}	44.8
20287.345	HC ₁₁ N	60–59	29.7
20292.487	HC ₃ ¹³ CC ₃ N	18–17	9.3
20294.271	HC ₄ ¹³ CC ₂ N	18–17	9.3
20303.946	HC ₇ N	18–17	9.3
20465.490	HC ₆ O	13–12 e	6.5
20465.504	HC ₆ O	12–11 e	6.5
20466.662	HC ₆ O	13–12 f	6.5
20466.676	HC ₆ O	12–11 f	6.5
20529.076	<i>i</i> -C ₉ H ₇ N	11 _{1,11} –10 _{1,10} , $F = 11-10$	6.1
20529.097	<i>i</i> -C ₉ H ₇ N	11 _{1,11} –10 _{1,10} , $F = 10-9$	6.1
20529.113	<i>i</i> -C ₉ H ₇ N	11 _{1,11} –10 _{1,10} , $F = 12-11$	6.1

Notes. Primary spectroscopic sources for molecular line frequencies: HC₇O and HC₆O – Mohamed et al. (2005), C₇O – Ogata et al. (1995), HC₁₁N – Travers et al. (1996), C₉H₇N and *i*-C₉H₇N – Kisiel et al. (2003), C₆O – Ohshima et al. (1995), CH₂(CN)₂ – Cox et al. (1985), C₄H₄N₂ – Kisiel et al. (1999), HC₅N – Bizzocchi et al. (2004), HC₇N and its isotopic species – McCarthy et al. (2000). The CH₂(CN)₂ and C₄H₄N₂ lines are blends of many hyperfine components due to the presence of two nitrogen nuclei.

els of 1–2 mK per channel. Targeted spectral line frequencies are shown in Table 1. We used line lists from the Cologne Database for Molecular Spectroscopy (Müller et al. 2001) and Jet Propulsion Laboratory Molecular Spectroscopy web pages⁷, augmented, where necessary, by our own extrapolations outside the laboratory data sets. The energy level quantum numbering schemes adopted here differ for the various molecules and are detailed in the primary spectroscopic references. For HC₇O, we obtained additional GBT KFPA data from the recent study of McGuire et al. (2017a).

3. RESULTS

Column densities were obtained using spectral line models constructed for each species, based on Gaussian (thermally broadened) opacity profiles (*e.g.* Nummelin et al. 2000). The cloud radial velocity (5.81 km s^{−1}) and Doppler FWHM (0.37 km s^{−1}) were obtained from a least-squares fit to the high signal-to-noise HC₇N $J = 18-17$ line (shown in Figure 4). The column density for each species was varied until the

⁷ <https://spec.jpl.nasa.gov/>

best fit to the observed spectral data was obtained; 1σ uncertainties were derived using Monte Carlo noise replication and re-fitting with 500 replications (as described by Cordiner et al. 2013). For species with no detectable emission, we adopted an approach similar to Loomis et al. (2016), by constructing a spectral model (with fixed radial velocity and line FWHM), and increasing the column density from zero until a χ^2 value of 2σ was reached. For species with multiple lines in different spectral windows, the fit was generated for all lines simultaneously, weighted by the RMS noise level in each window.

Rotational temperatures were taken from the literature where available: 5 K was adopted for HC_5N and 6 K for HC_7N based on Bell et al. (1998), and 10 K for HC_{11}N based on Bell et al. (1997) and Loomis et al. (2016). Although the kinetic temperature of TMC-1 CP has been well established at 10 K (e.g. Pratap et al. 1997), species with large dipole moments (such as the cyanopolynes and related asymmetric species with 3-9 C atoms) undergo rapid rotational cooling that can cause their rotational excitation temperatures (T_{rot}) to fall away from thermodynamic equilibrium. As discussed by Bell et al. (1998), the magnitude of this effect for the cyanopolynes is primarily dependent on the rotational constant (inverse of the molecule length). Thus, for species containing a chain of 6 or 7 C-atoms, we adopted $T_{\text{rot}} = 6$ K. For the remaining molecules, we adopted $T_{\text{rot}} = 10$ K. Our calculated column densities, abundances and upper limits are given in Table 2. The TMC-1 H_2 column density of $N_{\text{H}_2} = 10^{22} \text{ cm}^{-2}$ was taken from Cernicharo & Guelin (1987).

3.1. Carbon chain oxides

To obtain improved sensitivity to the cumulenone radical species HC_7O , our observational data (covering the $F = 17-16$ and $16-15$ e and f transitions) were combined with additional GBT data (covering the $F = 18-17$ and $17-16$ e and f transitions) from the study of McGuire et al. (2017a) for a total of eight HC_7O transitions, in the form of two pairs of hyperfine doublets. The data were rebinned to a common frequency resolution and transformed to the (LSR) velocity scale. At the resolution of our observed spectra, the hyperfine doublet structure of each line was not well resolved, so the mean rest frequency was used for each doublet. The average spectrum for the four doublets is shown in Figure 1, with a well-defined, statistically significant peak at the TMC-1 systemic velocity of 5.8 km s^{-1} (marked with a vertical dotted line). The integrated line intensity is $3.8 \pm 0.39 \text{ mK km s}^{-1}$, which corresponds to a 9.5σ detection.

A spectral line model was constructed to fit all eight HC_7O hyperfine components, shown in Figure 2. Allowing both the HC_7O column density (N) and radial velocity (v) to vary, the best-fitting model results were $N(\text{HC}_7\text{O}) = (7.8 \pm 0.9) \times 10^{11} \text{ cm}^{-2}$, and $v = 5.83 \pm 0.05 \text{ km s}^{-1}$.

Three possible formation mechanisms have been proposed for these carbon chain oxides. The observations reported here were originally motivated by the theoretical models of Cordiner & Charnley (2012) who considered the formation of C_6O , C_7O , HC_6O and HC_7O as a result of reactions between O atoms and carbon chain anions, as measured in the laboratory by Eichelberger et al. 2007. For reactions of oxygen with the polyne anions C_nH^- ($n = 2-7$), the most likely product channels are:

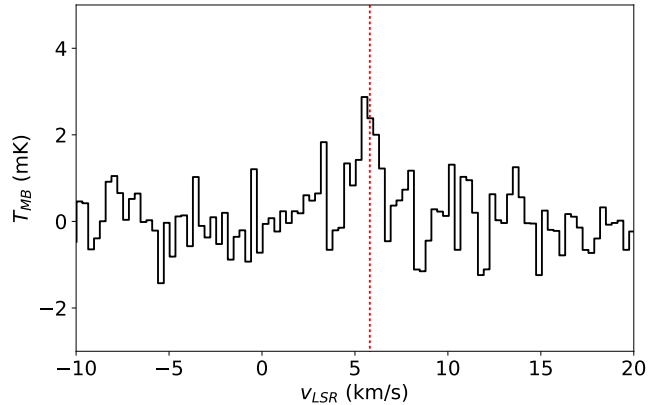
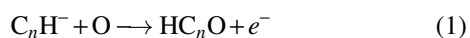


FIG. 1.— Average (in velocity space) of the four HC_7O doublets in our observed GBT spectra, showing a clear detection at the expected position of 5.8 km s^{-1} (dotted line).

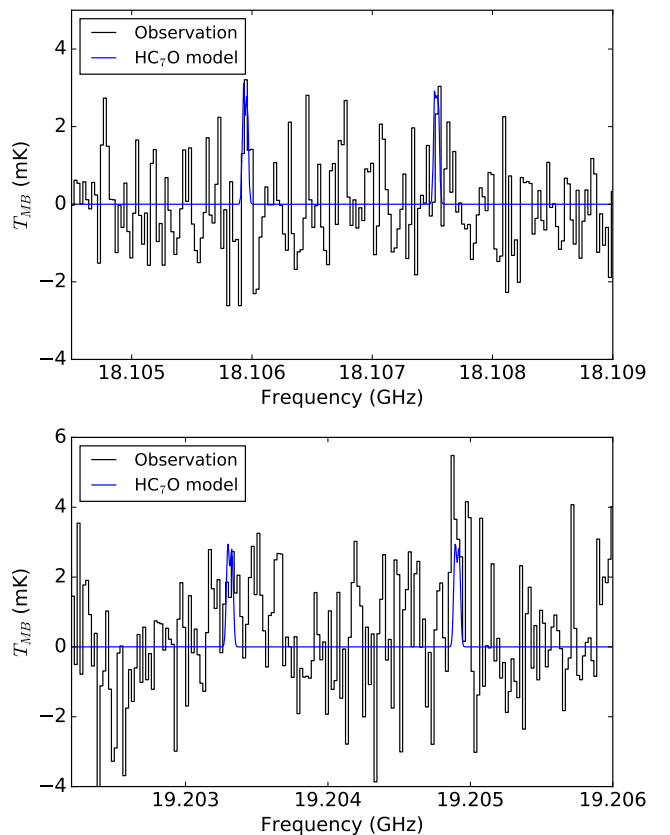
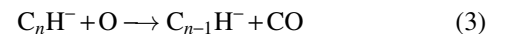
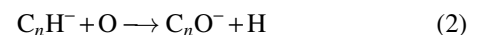


FIG. 2.— GBT spectra of the regions surrounding the two sets of observed HC_7O transitions (top panel: $17-16e$, $16-15e$, $17-16f$, $16-15f$; bottom panel: $18-17e$, $17-16e$, $18-17f$, $17-16f$). The same (best-fitting) HC_7O model is overlaid on each. Taken separately, these spectral features are of insufficient intensity to claim a detection, but taken together, they imply a detection of this molecule at the 9.5σ confidence level.



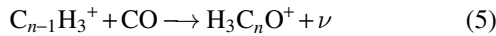
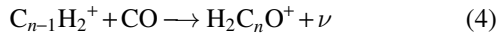
The chemical model for TMC-1 presented by Cordiner & Charnley (2012) predicted a maximum HC_7O column density of $\approx 1.5 \times 10^{13} \text{ cm}^{-2}$ at a chemical age of $t \approx 1 \times 10^5$ years, as well as potentially detectable abundances of the

TABLE 2
TMC-1 (CP) MOLECULAR COLUMN DENSITY/ABUNDANCE MEASUREMENTS AND UPPER LIMITS

Species	Name	T_{rot} (K)	N (cm $^{-2}$)	N/N_{H_2}
HC $_{11}$ N	Cyanodecapentayne	10	$< 7.4 \times 10^{10}$	$< 7.4 \times 10^{-12}$
HC $_7$ N	Cyanoheptatriyne	6	1.36×10^{13}	1.36×10^{-9}
HC $_3^{13}CC_3N$	^{13}C -Cyanohexatriyne	6	$(1.2 \pm 0.2) \times 10^{11}$	$(1.2 \pm 0.2) \times 10^{-11}$
HC $_4^{13}CC_2N$	^{13}C -Cyanohexatriyne	6	$(1.4 \pm 0.2) \times 10^{11}$	$(1.4 \pm 0.2) \times 10^{-11}$
HC $_5$ N	Cyanobutadiyne	5	5.3×10^{13}	5.3×10^{-9}
C $_6$ O	Hexacarbon monoxide	6	$< 5.2 \times 10^{10}$	$< 5.2 \times 10^{-12}$
C $_7$ O	Heptacarbon monoxide	6	$< 2.6 \times 10^{10}$	$< 2.6 \times 10^{-12}$
HC $_6$ O	1-oxo-hexa-1,3,5-triynyl	6	$< 1.5 \times 10^{11}$	$< 1.5 \times 10^{-11}$
HC $_7$ O	1-oxo-hepta-2,4,6-triynyl	6	$(7.8 \pm 0.9) \times 10^{11}$	$(7.8 \pm 0.9) \times 10^{-11}$
CH $_2$ (CN) $_2$	Malononitrile	10	$< 7.3 \times 10^{10}$	$< 7.3 \times 10^{-12}$
C $_4$ H $_4$ N $_2$	Pyrimidine	10	$< 4.2 \times 10^{13}$	$< 4.2 \times 10^{-9}$
C $_9$ H $_7$ N	Quinoline	10	$< 6.2 \times 10^{11}$	$< 6.2 \times 10^{-11}$
<i>i</i> -C $_9$ H $_7$ N	Isoquinoline	10	$< 9.4 \times 10^{11}$	$< 9.4 \times 10^{-11}$

other three molecules. This calculated maximum HC $_7$ O abundance is about a factor of 19 higher than the observed value reported here, and the modeled abundances of C $_6$ O, C $_7$ O and HC $_6$ O are also significantly higher than our derived upper limits. However, comparison of the observed HC $_7$ O abundance ($\approx 8 \times 10^{-11}$) with the TMC-1 model (Figure 4 of Cordiner & Charnley 2012) indicates that it can be reproduced at $t \approx 3 \times 10^5$ years, at which point the C $_6$ O and C $_7$ O abundances are also within the upper limits reported here. Although at $t \approx 3 \times 10^5$ years the HC $_6$ O abundance is comparable to that of HC $_7$ O, in conflict with our observed abundance limits, it should be noted that the Cordiner & Charnley (2012) model also over-predicted the C $_6$ H $^-$ abundance (by a factor of 6.7, compared with the observed value from Brünken et al. 2007). If the modeled C $_6$ H $^-$ abundance was less by a similar factor, then the predicted HC $_6$ O abundance would drop to just below our observed upper limit as a result of the close chemical relationship between these species.

McGuire et al. (2017a) considered the chemistry of the HC $_n$ O radicals ($n = 3 - 7$) based on an extension of the reactions suggested by Adams et al. (1989). In this case the cumulenone radicals are produced in radiative association reactions between hydrocarbon cations and CO:



followed by electron dissociative recombination of the ions. In a model for TMC-1, McGuire et al. (2017a) found that their observed HC $_5$ O column density and their HC $_7$ O upper limit were best reproduced at $t \approx 2 \times 10^5$ years. However, at this time HC $_4$ O was calculated to be about 37 times more abundant than observed, and HC $_6$ O was a factor of 3×10^{-3} below the observed upper limit.

It has been suggested that the presence of CCO and CCCO in TMC-1, as well as perhaps other carbon chain oxides, could originate in the injection of surface-formed cumulenone molecules from dust grains (Markwick et al. 2000). On cold dust grains, carbon atom additions, starting from HCO, could possibly lead to long cumulenone HC $_n$ O radicals that would form cumulenone molecules, H $_2$ C $_n$ O, following an H atom addition (cf. Charnley 1997). Following desorption, the cumulenone molecules would be protonated and the product ions subject to electron dissociative recombination reactions, leading to C $_n$ O and HC $_n$ O radicals, as well as H $_2$ C $_n$ O

molecules, all being present in the gas. Thus, in this case, the HC $_n$ O radicals would have both a grain-surface and a gas-phase origin. However, the non-detection of the propynonyl radical (HC $_3$ O) in TMC-1 (McGuire et al. 2017a), and consistently negative results from searches for propadienone (H $_2$ C $_3$ O) in molecular clouds, including TMC-1 (Irvine et al. 1988; Brown et al. 1992; Loison et al. 2016), tend to strongly disfavor this scenario.

Theoretical models for carbon chain oxide chemistry will require laboratory measurements of the rates and branching ratios of key formation reactions. Generally, the product distributions of electron dissociative reactions involving H $_m$ C $_n$ O $^+$ ions are important and, for anion chemistry, an assessment of the efficiency of the associative electron detachment (AED) channel (Reaction 1) would be very informative. Future deep searches in TMC-1 and elsewhere for these molecules will permit the elucidation of their exact formation pathways; for example, a detection of HC $_6$ O would help distinguish between the anionic and cationic formation mechanisms.

3.2. Cyanopolynes

3.2.1. HC $_{11}$ N confirmed non-detection

Our GBT K-band spectra support the results of Loomis et al. (2016): we searched at the frequencies of the higher-energy $J = 55 - 54$ and $J = 60 - 59$ transitions but found no evidence for any HC $_{11}$ N emission. Our spectra are shown in Figure 3 with a model based on the HC $_7$ N line FWHM and radial velocity, with the temperature and column density of Bell et al. (1997) overlaid. Our spectral line modeling implies a column density upper limit of 7.4×10^{10} cm $^{-2}$ (at 95% confidence), which is somewhat lower than the upper limit obtained by Loomis et al. (2016), and almost four times less than the value of 2.8×10^{11} cm $^{-2}$ claimed by Bell et al. (1997).

We performed our search for HC $_{11}$ N at the same coordinates as Loomis et al. (2016), so our combined results are consistent with a lack of HC $_{11}$ N at the TMC-1 cyanopolyne peak. It should be noted, however, that the detection claimed by Bell et al. (1997) was based on observations using a significantly larger (2.4') telescope beam, offset from the nominal cyanopolyne peak by about 1 s in RA and 9'' in declination. It is therefore conceivable that their larger, slightly offset telescope beam was sensitive to HC $_{11}$ N emission that was missed by the present study and that of Loomis et al. (2016). The previous detection of HC $_{11}$ N in TMC-1 therefore cannot be completely refuted until additional observations are performed,

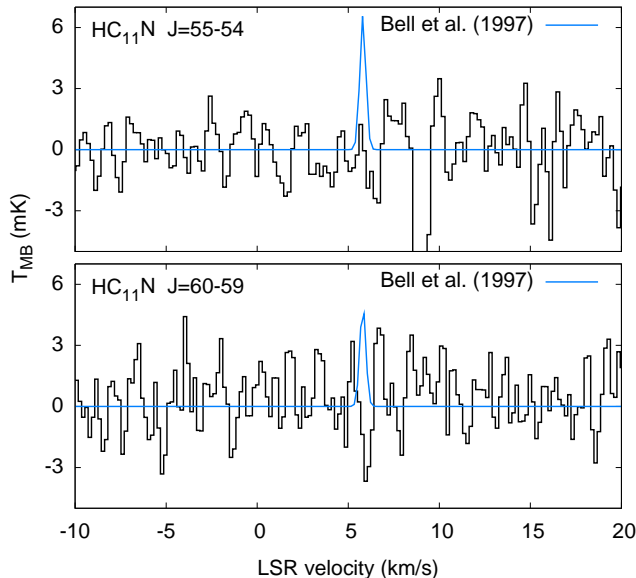


FIG. 3.— GBT K-band spectra surrounding two transitions of HC_{11}N . Predicted spectra based on the column density reported by Bell et al. (1997) are overlaid in blue.

ideally covering the same area on the sky as those made by Bell et al. (1997) using the NRAO 140-foot telescope.

3.2.2. New HC_7N isotopologues

The spectra shown in Figure 4 reveal the presence of the $J = 18 - 17$ lines of $\text{HC}_3^{13}\text{CC}_3\text{N}$ and $\text{HC}_4^{13}\text{CC}_2\text{N}$ at the $6-7\sigma$ level. This represents the first reported detection of individual isotopologues of HC_7N in any environment we are aware of. The only prior observation of ^{13}C -substituted HC_7N was in TMC-1 by Langston & Turner (2007) using the GBT, who stacked the spectra of various HC_7N isotopologues (with ^{13}C at different positions in the carbon chain), to obtain a mean $^{12}\text{C}/^{13}\text{C}$ ratio of 87_{-19}^{+37} for this molecule. We derive abundance ratios for the specific isotopologues $\text{HC}_7\text{N}/\text{HC}_3^{13}\text{CC}_3\text{N} = 110 \pm 16$ and $\text{HC}_7\text{N}/\text{HC}_4^{13}\text{CC}_2\text{N} = 96 \pm 11$. These values are notably high, and indicate depletion of ^{13}C relative to the local interstellar elemental $^{12}\text{C}/^{13}\text{C}$ ratio of 60-70 (Lucas & Liszt 1998; Milam et al. 2005). Depleted $^{12}\text{C}/^{13}\text{C}$ ratios have previously been observed in TMC-1 for the closely related molecules HC_3N and HC_5N , as well as CCH and CCS (Sakai et al. 2013). Modeling efforts are in progress to understand this isotopic depletion, which seems to be a common characteristic of carbon chains in cold interstellar gas (Yoshida et al. 2015; Araki et al. 2016).

Based on our new results, the depletion of ^{13}C in HC_7N (resulting in a higher $^{12}\text{C}/^{13}\text{C}$ ratio), seems to be stronger than for the shorter cyanopolynes. For HC_7N , our mean $^{12}\text{C}/^{13}\text{C}$ ratio is 103 ± 6 , compared with the mean value of 94 ± 6 for HC_5N (Taniguchi et al. 2016) and 70 ± 5 for HC_3N (Takano et al. 1998). However, it should be noted that previous studies have found the ratio to be significantly smaller for the carbon atom in the CN end-group than for the other C atoms along the chain (Taniguchi et al. 2016). Excluding the CN end-group, the mean ratios are 97 ± 7 for HC_5N and 77 ± 7 for HC_3N . Additional observations will be required to determine if this is also the case for HC_7N .

The current understanding regarding the origin of ^{13}C de-

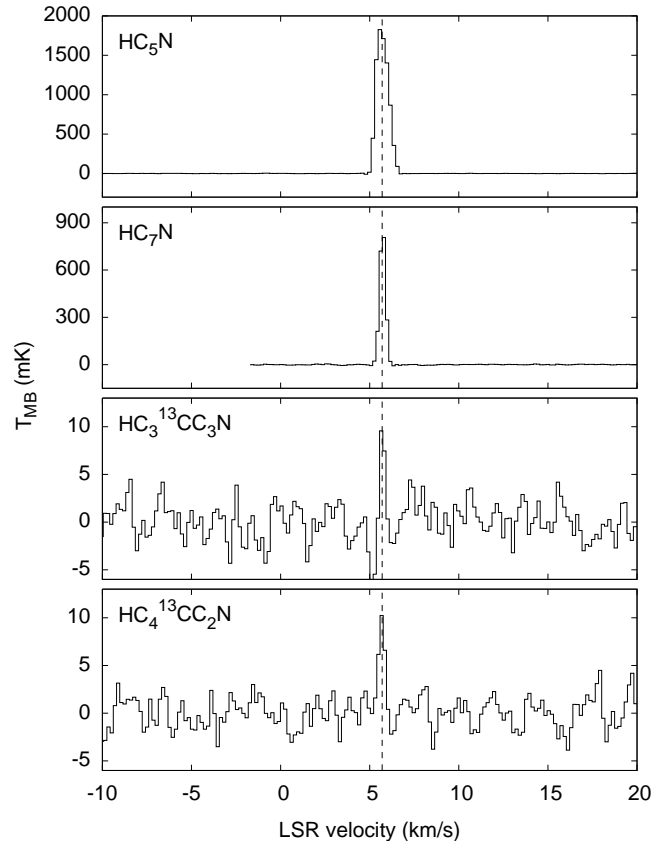


FIG. 4.— GBT K-band spectra showing detections of HC_5N , HC_7N , and its ^{13}C -substituted isotopologues $\text{HC}_3^{13}\text{CC}_3\text{N}$ and $\text{HC}_4^{13}\text{CC}_2\text{N}$.

pletion in carbon chain-bearing species is that it likely occurs due to gas-phase isotope exchange reactions, whereby ^{13}C is preferentially incorporated into other molecules. For instance, it is known that the $^{12}\text{C}/^{13}\text{C}$ ratio in (atomic) C^+ becomes depleted due to the incorporation of the heavier isotope into CO , through the exchange of ^{12}C and ^{13}C in the reaction between $^{13}\text{C}^+$ and ^{12}CO (Langer et al. 1984). It has thus been hypothesized that as gas-phase C^+ becomes depleted in ^{13}C , any molecules whose chemistry is closely linked with C^+ should also show isotopic depletion (Sakai et al. 2013).

It has been suggested that the analogous exchange reaction of $^{13}\text{C}^+$ with ^{12}CN could produce the observed (relative) ^{13}C enrichment of the CN group in cyanopolynes (Takano et al. 1998; Araki et al. 2016), but the viability of this mechanism has yet to be conclusively demonstrated in dense molecular clouds. Based on the relative similarities of the $^{12}\text{C}/^{13}\text{C}$ ratios in the different C atoms of HC_5N in TMC-1, Taniguchi et al. (2016) deduced that the main route to synthesizing the observed HC_5N is via hydrocarbon ion (plus N-atom) chemistry. The trend for lower ^{13}C fractions in progressively larger cyanopolynes is therefore indicative of a diminishing ^{13}C content in hydrocarbon ions of increasing size.

3.3. Nitrogen heterocycles

We searched for emission from multiple lines from quinoline ($\text{C}_9\text{H}_7\text{N}$), isoquinoline ($i\text{-C}_9\text{H}_7$) and pyrimidine ($\text{C}_4\text{H}_4\text{N}_2$) in TMC-1 and obtained strict (95% confidence) upper limits on their column densities of $6.2 \times 10^{11} \text{ cm}^{-2}$ and $9.4 \times 10^{11} \text{ cm}^{-2}$ for quinoline and isoquinoline, respectively,

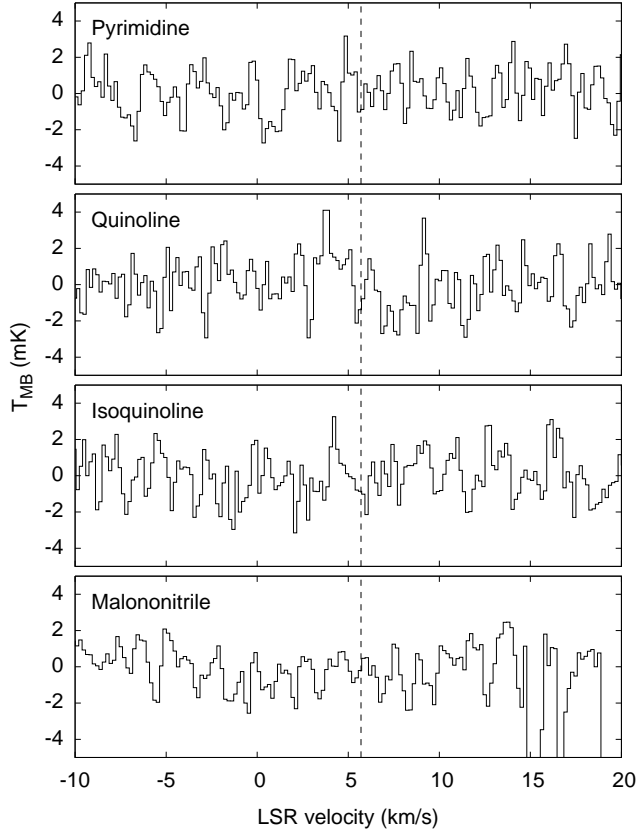


FIG. 5.— GBT K-band spectra showing non-detections of pyrimidine ($C_4H_4N_2$), quinoline (C_9H_7N), isoquinoline ($i-C_9H_7$) and malononitrile ($CH_2(CN)_2$).

and $4.2 \times 10^{13} \text{ cm}^{-2}$ for pyrimidine. [We also obtained an upper limit of $7.3 \times 10^{10} \text{ cm}^{-2}$ for malononitrile ($CH_2(CN)_2$.)]

4. CONCLUSIONS

We have performed deep searches for large organic molecules in TMC-1 with the GBT. Our data, when combined with that of McGuire et al. (2017a), allows us to confirm the previous tentative detection of HC_7O . The measured HC_7O column density and the derived upper limits for C_6O , HC_6O and C_7O place constraints on chemical models in which these molecules form through reactions involving negative and/or positively-charged hydrocarbon ions. We also confirm the previously reported non-detection of $HC_{11}N$ at the cyanopolyne peak by Loomis et al. (2016). We find that the detected ^{13}C isotopologues of HC_7N are depleted in ^{13}C . Reproduction of these $^{12}C/^{13}C$ ratios, as well as those measured in shorter carbon chain molecules (CCH, CCS, HC_3N and HC_5N), present a challenge for models of interstellar isotopic fractionation. Finally, our non-detections of nitrogen heterocycles in a cold molecular cloud complement previous non-detections of aromatic molecules in star-forming regions and in the envelopes of evolved stars. This raises the question: why have no aromatic compounds yet been detected by astronomical mm/submm spectroscopy? Most previous searches have involved targeting molecules in which the heteroatom, specifically N, is incorporated in an aromatic ring. While our derived abundance of pyrimidine is not particularly restrictive with regard to its possible presence in TMC-1, the recent detection of benzonitrile in TMC-1 by McGuire et al. (2017b) and of toluene in comet 67P/Churyumov-Gerasimenko Altwegg et al. (2017) suggests that interstellar chemistry may favor the presence of heteroatoms as functional side-groups, rather than within the ring structure. Future deep searches in TMC-1 with the GBT should provide further insights into the inventory of the heaviest interstellar molecules.

This work was supported by the Goddard Center for Astrobiology and NASA's Origins of Solar Systems and Exobiology programs.

REFERENCES

- Adams, N. G., Smith, D., Giles, K., & Herbst, E. 1989, *A&A*, 220, 269
 Altwegg, K., Balsiger, H., Bar-Nun, A., et al. 2016, *SciA*, 2, e1600285
 Altwegg, K., Balsiger, H., Berthelier, J. J., et al. 2017, *MNRAS*, 469, S130
 Araki, M., Takano, S., Sakai, N., et al. 2016, *ApJ*, 833, 291
 Bell, M. B., Feldman, P. A., Travers, M. J., et al. 1997, *ApJ*, 483, L61
 Bell, M. B., Watson, J. K. G., Feldman, P. A., & Travers, M. J. 1998, *ApJ*, 508, 286
 Bera, P. P., Lee, T. J., & Schaefer, H. F. 2009, *J. Chem. Phys.*, 131, 074303
 Biver, N., Bockelee-Morvan, D., Moreno, R., et al. 2015, *SciA*, 1, e1500863
 Bizzocchi, L., Degli Esposti, C., & Botschwina, P. 2004, *JMoSp*, 225, 145
 Brown, R. D., Cragg, D. M., Godfrey, P. D., et al. 1992, *OLEB*, 21, 399
 Brünken, S., Gupta, H., Gottlieb, C. A., McCarthy, M. C., & Thaddeus, P. 2007, *ApJ*, 664, L43
 Brünken, S., McCarthy, M. C., Thaddeus, P., Godfrey, P. D., & Brown, R. D. 2006, *A&A*, 459, 317
 Cernicharo, J. & Guelin, M. 1987, *A&A*, 176, 299
 Charnley, S. B. 1997, in *IAU Colloq. 161: Astronomical and Biochemical Origins and the Search for Life in the Universe*, Editrice Compositori, Italy, ed. C. Batalli Cosmovici, S. Bowyer, & D. Werthimer, Vol. 161, 89
 Charnley, S. B., Kuan, Y.-J., Huang, H.-C., et al. 2005, *AdSpR*, 36, 137
 Cochran, A. L., Lvasseur-Regourd, A.-C., Cordiner, M., et al. 2015, *SSRv*, 197, 9
 Cordiner, M. A., Buckle, J. V., Wirström, E. S., Olofsson, A. O. H., & Charnley, S. B. 2013, *ApJ*, 770, 48
 Cordiner, M. A. & Charnley, S. B. 2012, *ApJ*, 749, 120
 Cox, A. P., Kawashima, Y., Fliege, E., & Dreizler, H. 1985, *ZNatA*, 40, 361
 Ehrenfreund, P., Rasmussen, S., Cleaves, J., & Chen, L. 2006, *AsBio*, 6, 490
 Eichelberger, B., Snow, T. P., Barckholtz, C., & Bierbaum, V. M. 2007, *ApJ*, 667, 1283
 Gratier, P., Majumdar, L., Ohishi, M., et al. 2016, *ApJS*, 225, 25
 Herbst, E. & van Dishoeck, E. F. 2009, *ARA&A*, 47, 427
 Irvine, W. M., Brown, R. D., Cragg, D. M., et al. 1988, *ApJ*, 335, L89
 Jones, B. M., Zhang, F., Kaiser, R. I., et al. 2011, *PNAS*, 108, 452
 Kaifu, N., Ohishi, M., Kawaguchi, K., et al. 2004, *PASJ*, 56, 69
 Kisiel, Z., Desyatnyk, O., Pszczółkowski, L., Charnley, S. B., & Ehrenfreund, P. 2003, *JMoSp*, 217, 115
 Kisiel, Z., Pszczółkowski, L., López, J. C., et al. 1999, *JMoSp*, 195, 332
 Kuan, Y.-J., Yan, C.-H., Charnley, S. B., et al. 2003, *MNRAS*, 345, 650
 Langer, W. D., Graedel, T. E., Frerking, M. A., & Armentrout, P. B. 1984, *ApJ*, 277, 581
 Langston, G. & Turner, B. 2007, *ApJ*, 658, 455
 Loison, J.-C., Agúndez, M., Marcelino, N., et al. 2016, *MNRAS*, 456, 4101
 Loomis, R. A., Shingledecker, C. N., Langston, G., et al. 2016, *MNRAS*, 463, 4175
 Lucas, R. & Liszt, H. 1998, *A&A*, 337, 246
 Markwick, A. J., Millar, T. J., & Charnley, S. B. 2000, *ApJ*, 535, 256
 Materese, C. K., Nuevo, M., Bera, P. P., Lee, T. J., & Sandford, S. A. 2013, *AsBio*, 13, 948
 Materese, C. K., Nuevo, M., & Sandford, S. A. 2015, *ApJ*, 800, 116
 McCarthy, M. C., Levine, E. S., Apponi, A. J., & Thaddeus, P. 2000, *JMoSp*, 203, 75
 McElroy, D., Walsh, C., Markwick, A. J., et al. 2013, *A&A*, 550, A36
 McGuire, B. A., Burkhardt, A. M., Shingledecker, C. N., et al. 2017a, *ApJ*, 843, L28

- McGuire, B. A., Burkhardt, A. M., Shingledecker, C. N., et al. 2017b, submitted
- Milam, S. N., Savage, C., Brewster, M. A., Ziurys, L. M., & Wyckoff, S. 2005, *ApJ*, 634, 1126
- Mohamed, S., McCarthy, M. C., Cooksy, A. L., Hinton, C., & Thaddeus, P. 2005, *JChPh*, 123, 234301
- Müller, H. S. P., Thorwirth, S., Roth, D. A., & Winnewisser, G. 2001, *A&A*, 370, L49
- Mumma, M. J. & Charnley, S. B. 2011, *ARA&A*, 49, 471
- Nuevo, M., Materese, C. K., & Sandford, S. A. 2014, *ApJ*, 793, 125
- Nummelin, A., Bergman, P., Hjalmarsen, Å., et al. 2000, *ApJS*, 128, 213
- Öberg, K. I., Guzmán, V. V., Furuya, K., et al. 2015, *Natur*, 520, 198
- Ogata, T., Ohshima, Y., & Endo, Y. 1995, *JChS*, 117, 3593
- Ohishi, M. 2016, in *JPhCS*, Vol. 728, *JPhCS*, 052002
- Ohishi, M., Ishikawa, S.-I., Yamada, C., et al. 1991, *ApJ*, 380, L39
- Ohshima, Y., Endo, Y., & Ogata, T. 1995, *J. Chem. Phys.*, 102, 1493
- Pratap, P., Dickens, J. E., Snell, R. L., et al. 1997, *ApJ*, 486, 862
- Sakai, N., Takano, S., Sakai, T., et al. 2013, *JPCA*, 117, 9831
- Takano, S., Masuda, A., Hirahara, Y., et al. 1998, *A&A*, 329, 1156
- Taniguchi, K., Ozeki, H., Saito, M., et al. 2016, *ApJ*, 817, 147
- Tielens, A. G. G. M. 2008, *ARA&A*, 46, 289
- Travers, M. J., McCarthy, M. C., Kalmus, P., Gottlieb, C. A., & Thaddeus, P. 1996, *ApJ*, 469, L65
- Walsh, C., Loomis, R. A., Öberg, K. I., et al. 2016, *ApJ*, 823, L10
- Yoshida, K., Sakai, N., Tokudome, T., et al. 2015, *ApJ*, 807, 66